ISSN 0023-1584, Kinetics and Catalysis, 2008, Vol. 49, No. 4, pp. 599–605. © MAIK “Nauka/Interperiodica” (Russia), 2008.
Published in Russian in Kinetika i Kataliz, 2008, Vol. 49, No. 4, pp. 625–632.

III INTERNATIONAL CONFERENCE
“CATALYSIS: FUNDAMENTALS AND APPLICATIONS”

Modeling of a Radial-Flow Moving-Bed Reactor for Dehydrogenation of Isobutane[1]

Parisa Moghimpour Bijani and Saeed Sahebdelfar

Catalysis and Reaction Engineering Laboratory, Tehran University, P.O. Box 11465–4563, Tehran, Iran
Catalyst Research Group, Petrochemical Research and Technology Company, National Petrochemical Company,
P.O. Box 14358, Tehran, Iran
e-mail: s.sahebdel@npc-rt.ir

Received July 12, 2007

Abstract—A mathematical model for the performance of a radial-flow moving-bed reactor for dehydrogenation of light paraffins was developed. Assuming relevant kinetic expressions for the main reaction and catalyst deactivation, the kinetic parameters were obtained through lab-scale fixed-bed reactor testing using the integral method of analysis. The conversion was found to be a function of a dimensionless decay time, i.e., the ratio of a “catalyst deactivation time constant” to the residence time of the catalyst within the reactor. For a large dimensionless decay time (negligible catalyst decay), the performance equation approached that of a simple packed-bed reactor. The predictions of the model were compared with those of a commercial unit, and fair agreements were observed.

DOI: 10.1134/S0023158408040228

1. INTRODUCTION

Conventional processes for production of olefins such as steam crackers or FCC units alone do not satisfy the growing demand. Consequently, efficient catalytic dehydrogenation of light alkanes to the corresponding olefins is much sought as a means of converting relatively inert LPG hydrocarbons to reactive chemical feedstocks such as propylene and butenes. This has resulted in a number of commercial catalytic dehydrogenation processes.

The dehydrogenation of light alkanes can be represented as

$$C_nH_{2n+2} \longleftrightarrow C_nH_{2n} + H_2$$
$$\begin{cases} n = 3 \quad \Delta H^0_{298} = 124 \text{ kJ/mol} \\ n = 4 \quad \Delta H^0_{298} \approx 120 \text{ kJ/mol.} \end{cases} \qquad \text{(I)}$$

The reaction is reversible, endothermic, and accompanied by volume expansion. Therefore, higher temperatures and lower pressures shift it to completion. Higher temperatures, on the other hand, promote side reactions, coke formation, and catalyst deactivation. Using a suitable catalyst, the side reactions, which are often thermodynamically more favorable under reaction conditions, can be minimized. Typical commercial catalysts for dehydrogenation of light alkanes are either based on platinum or chromia.

Due to thermodynamic limitations, dehydrogenation of light alkanes is conducted at temperatures of around 600°C to achieve reasonable commercial yields. Under these conditions, catalyst deactivation is rapid and frequent catalyst regeneration is necessary. Some technologies operate under vacuum or in the presence of steam or even hydrogen to lower alkane partial pressure and to shift the reaction to olefin formation. The utilization of a diluent reduces the rate of coke formation and catalyst deactivation as well. A number of reaction-regeneration systems have been developed, which makes frequent catalyst regeneration possible [1–3].

In the *Oleflex* process of UOP [4], moving-bed reactors packed with a promoted, supported platinum catalyst are used. Figure 1 shows the scheme of one of the reactors in its longitudinal cross section. The reactor includes two perforated coaxial cylinders, between which the catalyst moves slowly downwards under action of gravity. The gaseous feed comprising a mixture of alkane and hydrogen enters from the bottom and crosses the catalyst bed, and the products leave the reactor from the other side. Radial flow reduces the pressure drop. Reactors operate adiabatically, and to achieve near isothermal conditions, three or four reactors are employed with interstage heaters.

The catalyst is progressively coked as it moves through the reactors. The catalyst leaving each reactor enters the next one, and the total residence time typically ranges between 2 and 7 days. The catalyst leaving the last reactor is send to the continuous catalyst regen-

---

[1] This article was submitted by the authors in English.

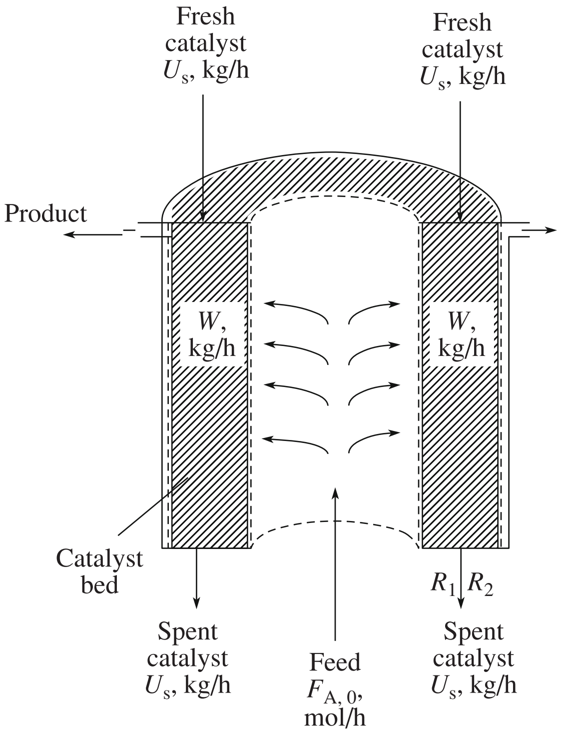

Fig. 1. Schematic representation of a radial moving-bed reactor.

eration (CCR) unit, where the coke is burnt, Pt redispersed, and the excessive moister is removed.

The Sn-promoted Pt catalysts undergo a "double mechanism" deactivation through coke deposition and sintering [5]. These catalyst can tolerate several percentage of coke build-up, preserving enough catalytic activity and allowing an "on stream" period of several hours/days before mandating catalyst regeneration [2, 5].

Although catalyst deactivation greatly complicates development of chemical processes and plant technology, it does not usually receive attention in academic research [6]. The important point in simulation of catalyst deactivation due to coke formation or poison deposition is to model these phenomena. While kinetic models for main reactions are well known as tools for process design, kinetic modeling of coke formation and catalyst deactivation are still considered to be too complicated to investigate by the accepted methods for the main reaction. Therefore, oversimplified empirical models with limited use of experimental works are derived which are often programmed very late and in the final stage of process development [7].

In the present work a simple model for performance of a radial-flow moving-bed reactor is developed. The applicability of the model is investigated for isobutane dehydrogenation, which is commercially operated by the above system. The proposed kinetic models for dehydrogenation reaction and catalyst deactivation are tested by a lab-scale fixed-bed reactor using two samples of commercial catalysts. The predictions of the model are compared to those of a commercial unit, and the limitations are discussed.

2. EXPERIMENTAL SECTION

The commercial Pt-Sn/Al_2O_3 catalyst samples (1.8 mm in diameter) were tested in a fixed-bed quartz reactor (15 mm id.) packed with a mixture of 2.2–2.8 g of catalyst and equal volume (3.0 ml) of quartz pellets of the same diameter as a diluent. The important operating conditions were selected close to industrial conditions as follows:

WHSV = 2.0–2.2 h^{-1} (referred to isobutane),
H_2/HC = 0.5–0.8 mol/mol,
Reaction temperature = 575°C,
Reaction pressure = atmospheric.

The reactor effluent was diluted with 45 ml/min of nitrogen before being injected to GC. The product was analyzed by a GC (Pu 4600 Phillips), equipped with TCD and FID detectors with He as the carrier gas. Isobutane conversion, isobutene selectivity, and the yield of the catalysate were calculated at different times.

The pressure of the commercial reactor is slightly above the atmosphere (about 2 atm, depending on the reactor number). A typical run took more than 100 h, which was in the range of the catalyst life cycle.

3. THEORETICAL BASIS

To begin with, consider the following reversible reaction:

$$A \rightleftharpoons B + H_2, \qquad \text{(II)}$$

where A and B represent the paraffin and olefin, respectively. There are good mechanistic kinetic models for dehydrogenation of paraffins on Pt-based catalysts [8]; however, for the present work simple yet accurate models suffice. Most previous studies have shown that the dehydrogenation reaction is first-order in paraffin concentration and negative half- to zeroth-order in hydrogen concentration [2]. Therefore, to incorporate the first-order dependence on paraffin concentration, the hydrogen-inhibition effect, and chemical equilibrium limitation, the following expression is assumed to represent kinetics of the reaction:

$$-r'_A = k_1 C_A - k_2 C_B C_{H_2} = k_1\left(C_A - \frac{C_B C_{H_2}}{K_{eq}}\right), \qquad (1)$$

where r'_A is the rate of disappearance of paraffin per catalyst weight; k_1 and k_2 are the rate constants of forward and backward reactions, respectively; K_{eq} is the equilibrium constant at reaction temperature; and C_i is the concentration of the species i. Larsson et al. [9] found that among several kinetic models tested for dehydrogenation of propane on Pt–Sn/Al_2O_3 catalysts, a simple power-law model of this type resulted in the best fit.

To account for catalyst deactivation, the reaction rate can be written in terms of activity as

$$-r'_A = k_1 a\left(C_A - \frac{C_B C_{H_2}}{K_{eq}}\right), \tag{2}$$

in which the catalyst activity, a, is defined as

$$a(t) = \frac{-r'_A(t)}{-r'_A(t=0)} = \frac{-r'_A}{-r'_{A,0}}. \tag{3}$$

Considering the volume change of the reaction, following rather involved algebraic manipulations, one arrives at the following expression for reaction rate in terms of paraffin conversion:

$$-r'_A = \frac{k_1 a C_{A,0}(X_{A,eq} - X_A)(\alpha + \beta X_A)}{(1 + \varepsilon_A X_A)^2}, \tag{4}$$

in which

$$\alpha = \frac{X_{A,eq} + (\Theta_H + \Theta_B) + \Theta_H\Theta_B(1 - \varepsilon_A + \varepsilon_A X_{A,eq})}{(\Theta_H + X_{A,eq})(\Theta_B + X_{A,eq})}, \tag{5}$$

$$\beta = \frac{(1 + \varepsilon_A X_{A,eq} - X_{A,eq}) + \varepsilon_A X_{A,eq}(\Theta_H + \Theta_B) + \varepsilon_A\Theta_H\Theta_B}{(\Theta_H + X_{A,eq})(\Theta_B + X_{A,eq})}, \tag{6}$$

where Θ_H and Θ_B are hydrogen/paraffin and olefin/paraffin molar ratios initially (or in the feed), respectively; X_A is paraffin conversion, $X_{A,eq}$ is the equilibrium conversion under reaction conditions, and ε_A is the volume expansion factor. When $X_{A,eq}$ approaches unity (i.e., to that of irreversible reactions), the parameters α and β approach unity and ε_A, respectively.

From a paraffin mole balance on the cylindrical element within the reactor bed (Fig. 2), one obtains, successively,

$$-dF_A + r'_A dW = 0, \tag{7}$$

$$dF_A = d[F_{A,0}(1 - X_A)] = -F_{A,0}dX_A, \tag{8}$$

$$\frac{dX_A}{-r'_A} = \frac{dW}{F_{A,0}}, \tag{9}$$

where $F_{A,0}$ is the molar flow rate of paraffin, W is the weight of the catalyst, and the subscript 0 refers to the inlet conditions to the reactor. Equation (9) represents the design equation of the moving-bed reactor. The final form depends on the geometry of the volume element. For the system under consideration,

$$dW = \rho_b 2\pi r dr dz, \tag{10}$$

where ρ_b is the bulk density of the catalyst.

Now, assume the following rate law for catalyst deactivation:

$$-\frac{da}{dt} = k_d a, \tag{11}$$

where k_d is deactivation rate constant. This form of decay law has been used for dehydrogenation of light paraffin on Pt-based catalysts by several authors [10, 11].

The catalyst residence time within the reactor is

$$t = \frac{W}{U_s} = \frac{\rho_b V}{U_s} = \rho_b\frac{\pi(R_2^2 - R_1^2)z}{U_s} \Rightarrow dt = m dz, \tag{12}$$

where U_s is the mass flow rate of the catalyst; R_1 and R_2 are the inner and outer radii of the moving-bed, respectively; and

$$m = \rho_b\frac{\pi(R_2^2 - R_1^2)}{U_s} \tag{13}$$

is the reciprocal of the linear velocity of the catalyst within the bed. From Eqs. (11) and (12), one obtains the rate of catalyst deactivation within the catalyst bed as

$$-da = k_d a dt = k_d m a dz. \tag{14}$$

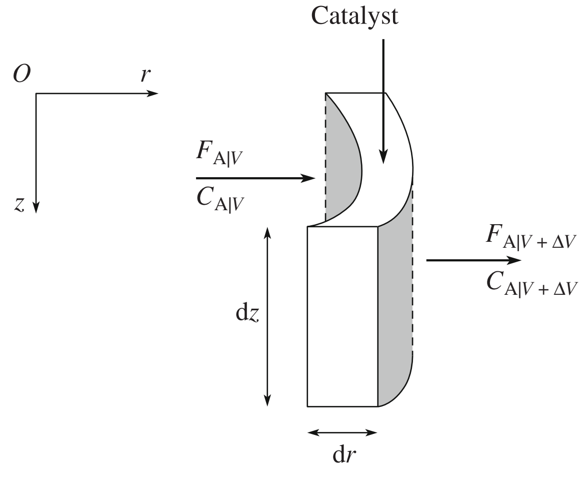

Fig. 2. Radial element in the catalyst bed.

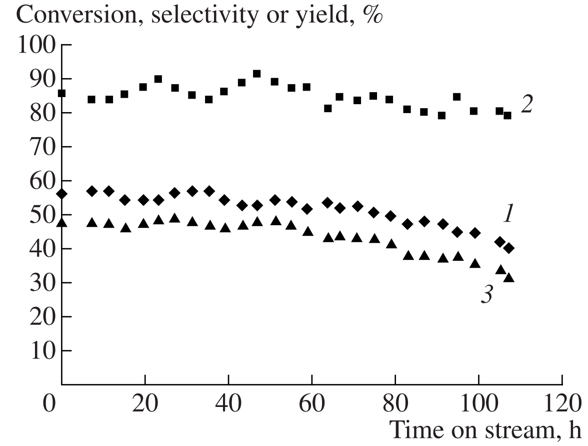

Fig. 3. Typical time-on-stream behavior for Catalyst A (WHSV = 2 h^{-1}, H_2/HC = 0.5 mol/mol): (*1*) isobutane conversion, (*2*) isobutylene selectivity, and (*3*) isobutylene yield.

If the catalyst activity at the reactor entrance ($z = 0$) is a_0, from Eq. (14) one obtains

$$a(z) = a_0 \exp\left(-k_\text{d}\rho_\text{b}\pi\frac{(R_2^2 - R_1^2)}{U_\text{s}}z\right). \tag{15}$$

Equation (15) shows the variation of catalyst activity along the bed. Combining Eqs. (4), (9), and (15) and integrating along bed height, h, one obtains

$$\frac{F_{\text{A},0}}{2\pi\rho_\text{b}k_1C_{\text{A},0}}\int\limits_{X_\text{A, in}}^{X_\text{A, out}}\frac{(1+\varepsilon_\text{A}X_\text{A})^2}{(X_\text{A, eq}-X_\text{A})(\alpha+\beta X_\text{A})}\text{d}X_\text{A} = \int\limits_0^h\int\limits_{R_1}^{R_2} a_0\text{e}^{-mk_\text{d}z}r\text{d}r\text{d}z. \tag{16}$$

Noting

$$W = \rho_\text{b}\pi(R_2^2 - R_1^2)h, \tag{17}$$

it follows that

$$\begin{aligned}&\frac{(\beta-\varepsilon_\text{A}\alpha)^2}{\beta(\alpha+\beta X_\text{A, eq})}\ln\left(\frac{\alpha+\beta X_\text{A, out}}{\alpha+\beta X_\text{A, in}}\right)\\ &-\frac{\beta(1+\varepsilon_\text{A}X_\text{A, eq})^2}{(\alpha+\beta X_\text{A, eq})}\ln\left(\frac{X_\text{A, eq}-X_\text{A, out}}{X_\text{A, eq}-X_\text{A, in}}\right)\\ &-\varepsilon_\text{A}^2(X_\text{A, out}-X_\text{A, in})\\ &=\frac{k_1a_0C_{\text{A},0}U_\text{s}\beta}{k_\text{d}F_{\text{A},0}X_\text{A, eq}}\left(1-\exp\left(\frac{-k_\text{d}W_\text{c}}{U_\text{s}}\right)\right),\end{aligned} \tag{18}$$

where $X_\text{A, in}$ and $X_\text{A, out}$ represent the conversion at the inlet and outlet relative to the feed of the first reactor, respectively. Equation (18) gives the paraffin conversion in terms of feed composition and operating conditions. For the first reactor, $X_\text{A, in}$ equals zero.

One observes that the argument of the exponential function in Eq. (18) is a Damkohler number for catalyst decay. Similarly, the term factored out from the right-hand-side (excluding β) is the ratio of the Damkohler number for the main reaction to that for catalyst decay.

4. RESULTS AND DISCUSSION

Figure 3 shows a typical long-term time-on-stream performance of catalysts from experimental runs. While the selectivity remains rather constant, activity drops smoothly as implied by drop of conversion. Therefore, olefin yield closely parallels paraffin conversion and the latter can be considered as a good measure of the overall performance of the catalyst during its lifetime. The stable selectivity depicted in Fig. 3 is typical of Sn-promoted platinum catalysts and can be explained in geometric terms by the dilution of Pt ensembles by Sn. This dilution greatly reduces the activity toward reactions that require a large ensemble of Pt-atoms to constitute active sites, such as hydrogenolysis and coking [2]. Additionally, the carbon deposited during reaction acts the role of inactive species that inhibits undesired reactions. Therefore, although coke deposition adversely affects catalyst activity, it exhibits some beneficial effects on olefin selectivity.

4.1. Kinetic parameters. To test the validity of the kinetics assumed and to obtain the kinetic parameters required for Eq. (18) from experimental data, an integral method of analysis can be used. According to the kinetics assumed in Eqs. (2) and (11) and the performance equation of the tubular packed-bed reactor, it can be shown that for a fixed-bed reactor

$$\begin{aligned}k_1\tau'\text{e}^{-k_\text{d}t} = \beta^{-1}\Bigg[&\frac{(\beta-\varepsilon_\text{A}\alpha)^2}{\beta(\alpha+\beta X_\text{A, eq})}\ln\left(\frac{\alpha+\beta X_\text{A}}{\alpha}\right)\\ &-\frac{\beta(1+\varepsilon_\text{A}X_\text{A, eq})^2}{(\alpha+\beta X_\text{A, eq})}\ln\left(\frac{X_\text{A, eq}-X_\text{A}}{X_\text{A, eq}}\right)-\varepsilon_\text{A}^2X_\text{A}\Bigg]\end{aligned} \tag{19}$$

or, upon taking the logarithm of both sides,

$$\begin{aligned}\ln(k_1\tau') - k_\text{d}t = \ln\Bigg[\beta^{-1}\Bigg[&\frac{(\beta-\varepsilon_\text{A}\alpha)^2}{\beta(\alpha+\beta X_\text{A, eq})}\ln\left(\frac{\alpha+\beta X_\text{A}}{\alpha}\right)\\ &-\frac{\beta(1+\varepsilon_\text{A}X_\text{A, eq})^2}{(\alpha+\beta X_\text{A, Õ-t})}\ln\left(\frac{X_\text{A, eq}-X_\text{A}}{X_\text{A, eq}}\right)-\varepsilon_\text{A}^2X_\text{A}\Bigg]\Bigg] = f(X_\text{A}),\end{aligned} \tag{20}$$

in which τ', the ratio of catalyst weight per volumetric feed flow rate, is a capacity factor known as the weight-time.

Equation (20) proposes a method for testing the kinetic expressions employed. To obtain equilibrium conversions, the equilibrium constant was calculated from the free energy of formations of the species involved in the reaction from the literature (for exam-

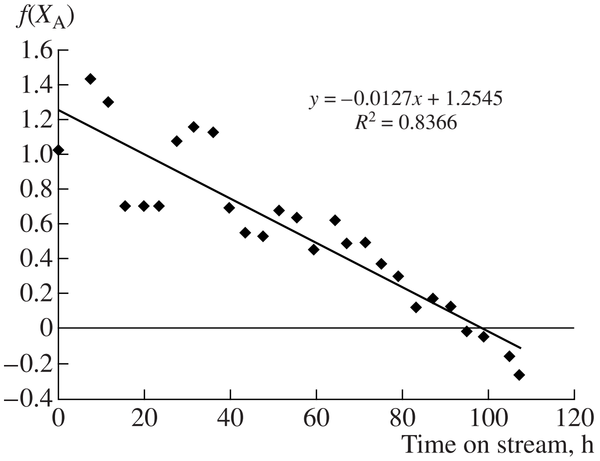

Fig. 4. Testing Eq. (20) using experimental data for Catalyst A (WHSV = 2 h^{-1}, H_2/HC = 0.5 mol/mol).

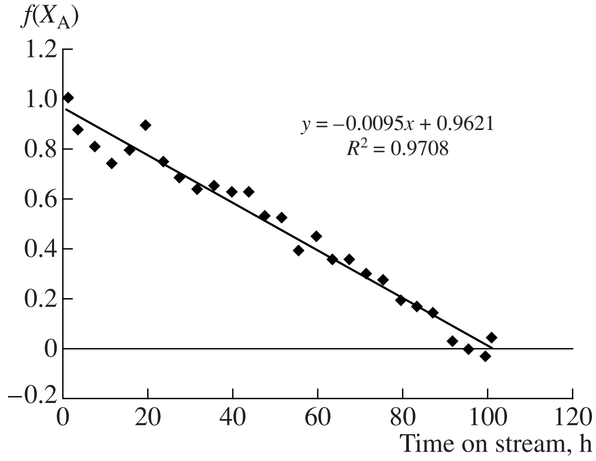

Fig. 5. Testing Eq. (20) using experimental data for Catalyst B (WHSV = 2.2 h^{-1}, H_2/HC = 0.8 mol/mol).

ple, [12]). Figures 4 and 5 show plots of Eq. (20) based on experimental concentration-time data for two different commercial catalyst samples.

As is observed, the kinetic models adequately predict the trend in the reduction of conversion and deactivation for both catalysts. This confirms the validity of a first-order decay law for the range of interest. The scatter in experimental data is more pronounced at early time on stream. This is due to the fact that the reactor effluent is close to equilibrium, and any error in calculating conversions is magnified due to the logarithmic term in the right-hand-side of Eq. (20). The observed fluctuations are damped out with increasing time on stream, because as the catalyst deactivates and the reaction departs from chemical equilibrium. The slopes and intercepts of the two lines are close and consistent, implying similar performances of the two catalysts.

Plots similar to Figs. 4 and 5 provide a convenient screening test of dehydrogenation catalysts in terms of activity and stability. Accordingly, catalyst A is more active but less stable than catalyst B. This tendency is common within catalysts of the same family; that is, the higher the catalyst activity, the more rapid its decay rate under similar operating conditions. As the commercial plant data were those of isobutane dehydrogenation using catalyst A, Fig. 4 is used to obtain kinetic parameters for scale-up. From the slope and intercept of Fig. 4, one obtains $k_d = 0.0127$ h^{-1} and $k_1\tau' = 3.51$. Considering the operating conditions ($\tau' = 0.972$ kg h/m^3), the rate constant is found to be $k_1 = 3.61$ m^3/(kg h).

Equation (11) is indicative of independent deactivation kinetics [13]. This implies that deactivation may be caused both by hydrocarbon products and reactants, the total concentration of which is nearly independent of paraffin conversion. Similar behavior is observed in certain other hydrocarbon conversion reactions such as isomerization and cracking [13].

Implicit in derivation of Eq. (19) is a pseudo-steady-state assumption. This assumption should be valid as the deactivation rate is very slow such that conditions change slowly enough for the system to be at steady state at any instant of time.

4.2. Mass transfer limitation effects. The influence of mass transfer limitations on the reaction can be examined, for example, through Mears and Weisz–Prater analyses for external and internal mass transfer limitations, respectively. Knowing the kinetic parameters from the previous section, the reaction rate can be obtained at any point using Eq. (4). The effective diffusivity and mass transfer coefficient can be estimated from appropriate correlations given in the literature. In this way, one observes based on maximum reaction rate $C_M = 7.4 \times 10^{-7} \ll 0.15$ and $C_{WP} = 0.09 \ll 1$, confirming working under the kinetic regime.

The Weisz–Prater parameter, however, is not small enough to ensure negligible intraparticle diffusion limitation throughout operation. Coking might cause a significant additional diffusion limitation. The presumed series-parallel deactivation mentioned in the previous section as well as cross-sectional examination of the coked catalysts implies that uniform coke deposition occurs. On the other hand, a significant diffusion limitation (for example, through pore-mouth plugging) could result in a shifting-order decay law, which is not confirmed by experimental observations. Consequently, mass transfer limitations should be negligible throughout the useful life of the catalyst in both scales and the reaction rate and kinetic parameters represent the intrinsic ones. This reduces the complexities that often arise in scale-up due to the difference in extent of resistances in the two scales.

4.3. Testing the model. The table compares the predicted and practical values of isobutane conversion for each reactor of the commercial plant. As is observed, the predicted overall conversion is very close to the real

Comparison of the industrial results with the model

	Reactor 1	Reactor 2	Reactor 3	All reactors
Predicted conversion (reactor outlet)	0.25	0.17	0.10	0.52
Conversion in industrial reactor (reactor outlet)	0.20	0.165	0.135	0.5
Activity of outlet catalyst	0.65	0.4	0.23	0.23

value. However, the conversion in the first reactor is overestimated, while that in the third one is underestimated. The prediction for the second reactor shows the best agreement. This might be attributed to the fact that to achieve nearly the same level of conversion per reactor, in commercial practice, the average temperature increases slowly from the first to the last reactor. The average temperature used in conversion calculations should be slightly higher than that for the first and slightly lower than that for the third reactor. More accurate results could be obtained through performing lab-scale tests at the average temperature of each reactor.

Also, the activity of the catalyst leaving each reactor is presented. As it is observed, the catalyst leaving the last reactor still retains one-fourth of its activity. Due to economic and technical considerations, the catalyst is sent to the regeneration unit before complete deactivation. In other words, the decrease in activity is not too significant and simple expressions such as first-order decay law could be adequate to describe the deactivation behavior.

In the limiting case when the catalyst activity is constant along the catalyst bed, one expects that the performance equation of the moving-bed reactor would reduce to that of a fixed-bed reactor in the absence of catalyst deactivation. Noting Eq. (18), one observes that the argument of the exponential function is the ratio of two characteristic times: the residence time of the catalyst within the reactor to the "deactivation time." When the residence time is very small compared with the deactivation time (that is, $k_1W/U_s > 0$), the activity is the same throughout the reactor and equals that for the catalyst at the entrance and the performance equation must approach that of a plug reactor. In this case, assuming $a_0 = 1$, the right-hand-side term of Eq. (18) can be written successively as

$$\frac{k_1 C_{\mathrm{A},0} U_{\mathrm{s}} \beta}{k_{\mathrm{d}} F_{\mathrm{A},0}}\left(1-\exp\left(\frac{-k_{\mathrm{d}} W}{U_{\mathrm{s}}}\right)\right) \qquad (21)$$

$$\sim \frac{k_1 C_{\mathrm{A},0} U_{\mathrm{s}} \beta}{k_{\mathrm{d}} F_{\mathrm{A},0}}\left(1-\left(1-\frac{k_{\mathrm{d}} W}{U_{\mathrm{s}}}\right)\right) = k_1\beta\left(\frac{C_{\mathrm{A},0} W}{F_{\mathrm{A},0}}\right) = k_1\tau'\beta,$$

where upon substituting into Eq. (18), one obtains Eq. (19) (with $k_{\mathrm{d}} = 0$ and $X_{\mathrm{A,\,in}} = 0$). Thus, the reactor behaves like a fixed-bed reactor being packed with fresh catalyst.

4.4. Influence of intrabed temperature profile. To solve the model analytically, the reactors were assumed to be isothermal operating under some average temperature. This is nearly the case for the lab-scale packed-bed reactor employed for determination of kinetic parameters. However, the commercial moving-bed reactors operate adiabatically and can exhibit a radial temperature decline. There should exist also a much less pronounced axial temperature change, which originates from catalyst deactivation.

Assabumrungrat et al. [14] obtained an activation energy of 62.7 kJ/mol for dehydrogenation of propane on Pt–Sn–K/γ-Al_2O_3 catalysts. Aguilar–Rios et al. [11] obtained 92 kJ/mol for the same reaction in the presence of hydrogen on both Pt/$MgAl_2O_4$ and Pt–Sn/$MgAl_2O_4$ catalysts. Both activation energies fall within the range of low activation energy reactions.

To account for the influence of bed temperature profiles on reactor performance, one can apply the model explicitly to cylindrical elements of width Δr and height Δz within which the temperature can be considered as constant. Scanning the reactor from the top element in the inner wall side to the lowest element in the outer wall side of the bed will result in concentration, activity, and temperature profiles across the reactor from which conversion can be obtained. The temperature increase per element can be obtained by energy balance considerations. Activation energy of the main reaction and catalyst decay can be obtained by Arrhenius plots of the rate constants obtained from plots such as Figs. 4 and 5.

4.5. Final remarks. To be applicable for scale-up, the formulations outlined here need only the reaction temperature and hydrogen-to-hydrocarbon ratio of the feed to be the same at the two scales. In this case, the corresponding rate constants are equal and the results from the lab-scale reactor are applicable to a commercial reactor. Temperature affects the rate constant of reactions as well as the equilibrium constant. The deactivation rate constant, on the other hand, in addition to temperature, depends on the hydrogen concentration. The concentration of hydrogen can be assumed to be constant through the reactor (i.e., method of excess), and therefore, no attempt is made to incorporate the concentration of hydrogen in the catalyst decay law. Hence, the deactivation rate constant is dependent upon the hydrogen-to-hydrocarbon ratio, which consequently should be the same at both scales. Other variables should not necessarily be the same at the two scales. For example, while the lab-scale reactor is atmospheric, the commercial plant operates at about 2 bar. Also, it should be noted that the commercial reactors operate adiabatically rather than isothermally. The temperature drop decreases successively from the first reactor to the last reactor, while the average temperature increases slowly from the first to the last reactor. Better results could be achieved by obtaining the effect of temperature on rate constants using numerical methods.

In the present work, no attempt has been made to develop a kinetic model for the main reaction and deactivation kinetics. The kinetic relations employed are simple, single-parameter ones, whose parameters can be readily calculated using lab-scale test runs.

5. CONCLUSIONS

This study showed the effect of important operating parameters on the performance of a moving-bed reactor in dehydrogenation of light alkanes. The alkane conversion was found to be a function of a dimensionless decay time, i.e., the ratio of two characteristic times, the “catalyst deactivation time constant” to the residence time of the catalyst within the reactor. The applicability of simple-to-treat, single-parameter kinetic expressions in describing the kinetics was verified. The observed catalyst decay kinetics was considered as an indication for series-parallel catalyst deactivation to occur. The correlations developed can be used for screening dehydrogenation catalysts. It is shown that in commercial practice the catalyst sent to the regeneration system still retains a considerable portion of its activity.

ACKNOWLEDGMENTS

One of the authors (P.M.B.) wishes to thank the Research and Technology Company of National Petrochemical Company (NPC–RT) for financial support. The technical guidance of Dr. Farhad Khorasheh (Sharif University of Technology) and Mr. Kamran Ganji (Kimia Petrochemical Company) is acknowledged with thanks.

REFERENCES

1. Bahsin, M.M., McCain, J.H., Vora, B.V., Imai, T., and Pujado, R.R., *Appl. Catal., A*, 2001, vol. 221, p. 379.
2. Resasco, D.E, in *Encyclopedia of Catalysis*, Horvath, I.T.N.Y., Ed., New York: Wiley, 2003, vol. 3, p. 49.
3. Buonomo, F., Sanfilippo, D., and Trifiro, F., in *Handbook of Heterogeneous Catalysis*, Ertl, G., Knoezinger, H., and Weitkamp, J., Eds., New York: Wiley–VCH, 1997, vol. 4.
4. Pujado, P.R. and Vora, B.V., *Hydrocarbon Process.*, March 1990, p. 65.
5. Sanfilippo, D. and Miracca, I., *Catal. Today*, 2006, vol. 111, p. 133.
6. Moulijn, J.A., van Diepen, A.E., and Kapteijn, F., *Appl. Catal., A*, 2001, vol. 212, p. 3.
7. Froment, G.F., *Appl. Catal., A*, 2001, vol. 212, p. 117.
8. Cortright, R.D., Levin, P.E., and Dumesic, J.A., *Ind. Eng. Chem. Res.*, 1998, vol. 37, p. 1717.
9. Larsson, M., Henriksson, N., and Andersson, B., *Appl. Catal., A*, 1998, vol. 166, p. 9.
10. Ohta, M., Ikeda, Y., and Igarashi, A., *Appl. Catal., A*, 2004, vol. 266, p. 229.
11. Aguilar-Ríos, G., Salas, P., Valenzuela, M.A., Armendáriz, H., Wang, J.A., and Salmones, J., *Catal. Lett.*, 1999, vol. 60, p. 21.
12. Yaws, C.Y., *Chemical Properties Handbook: Physical, Thermodynamic, Environmental, Transport, Safety, and Health Related Properties for Organic and Inorganic Chemicals*, New York: McGraw-Hill, 1999.
13. Levenspiel, O., *Chemical Reaction Engineering*, New York: Wiley, 1999.
14. Assabumrungrat, S., Jhoraleecharnchai, W., Praserthdam, P., and Goto, S., *J. Chem. Eng. Jpn.*, 2000, vol. 33, p. 529.